Available online at www.sciencedirect.com
SCIENCE DIRECT®
Estuarine, Coastal and Shelf Science 60 (2004) 165–177
ESTUARINE COASTAL AND SHELF SCIENCE
www.elsevier.com/locate/ECSS

Patterns and dynamics of coastal waters in multi-temporal satellite images: support to water quality monitoring in the Archipelago Sea, Finland

Anne Erkkilä[a,*], Risto Kalliola[b]

[a]*Department of Geography, University of Turku, c/o Center for Maritime Studies, P.O. Box 181, FIN-28101 Pori, Finland*
[b]*Department of Geography, University of Turku, FIN-20014 Turku, Finland*

Received 7 May 2003; accepted 30 November 2003

Abstract

The Archipelago Sea in the northern Baltic is a coastal region with a highly dynamic water flow regime, where the need for a methodology to monitor water quality accurately is encountered. In order to contribute to the development of an appropriate strategy to meet this need, the dynamics of the surface waters in the region were analysed using data from six Landsat TM/ETM+ images from the late 1990s. Single images were enhanced by principal component transformation and multi-temporal image combination was based on unsupervised classification. The visual patterns discernible in the single images as well as the classification result of the multi-temporal data were compared with the reference data from long-term water quality analyses (Secchi disk depth and chlorophyll-*a*). The satellite images confirmed dynamic surface flow patterns in the region, indicating gradual and abrupt gradients in water quality, flow directions and forms. These patterns suggest short-term variability in the surface water quality within the region, presenting a challenge for water monitoring. The average Secchi depths increased gradually from the mainland coast until ca. 3–5 m near the open sea. The spatial distribution of chlorophyll-*a* was found to be more homogeneous, ca. 2–4 $\mu g\, l^{-1}$. The importance of evaluating the location of an in situ sampling site in relation to the surrounding hydrographic realm is pronounced in regions where field sampling and other monitoring methods remain insufficient in their ability to reflect water quality patterns credibly. In such areas, accurate and cost-effective water quality monitoring and forecasting require an integrated monitoring system, consisting of space and airborne surveillance, field surveys and hydrodynamic modelling.

Keywords: water quality; environmental monitoring; remote sensing; Secchi disk depth; chlorophyll-*a*; Baltic Sea

1. Introduction

Water quality monitoring is crucial for any effort to produce information in support of water conservation and decision-making. Monitoring normally needs to be carried out as cost-effectively as possible relative to the type of information needed. Often it is expected that water quality should be shown with high accuracy in all places, in spite of the fact that direct observations can only be done in a limited number of locations. The need for an effective operational monitoring system that is able to solve the contradiction between cost-effectiveness and spatially comprehensive coverage is particularly pronounced in areas with variable seashore and water flow conditions.

The Archipelago Sea of Southwestern Finland provides an extreme example of a fragmented coastal region with its highly irregular shoreline form and complex hydrodynamic realm. Situated in the northern margins of the Baltic Sea proper, the Archipelago Sea contains thousands of islands in various sizes, forms and spatial assemblages, forming a complex transition from the continent to the open sea. The archipelago district is an important recreational area used by boaters and it has a dense settlement of summer residences. The mainland beyond the Archipelago Sea has a population of nearly half a million; boasting a variety of industries and

* Corresponding author.
E-mail addresses: anne.erkkila@utu.fi (A. Erkkilä), risto.kalliola@utu.fi (R. Kalliola).

0272-7714/$ - see front matter
doi:10.1016/j.ecss.2003.11.024

intensive agriculture with significant fertilizer input. The Archipelago Sea is also the major fish farming area in Finland (Kirkkala et al., 1998).

During recent decades, eutrophication has been the primary environmental concern in this region (Bonsdorff et al., 1997). According to residents of the region, water transparency has decreased significantly and at the same time green algae have been augmenting along the shoreline. Environmental monitoring efforts also confirm that accelerating eutrophication is a reality in the Archipelago Sea and in the nearby areas of open sea (Kirkkala et al., 1998; Hänninen et al., 2000). An increase in cyanobacterial blooming has been detected in the Baltic Sea especially in the 1990s, including species of *Nodularia*, *Aphanizomenon* and *Anabaena* (Kahru et al., 1994; Finni et al., 2001). The extensive accumulations observed in the late summers of 1997 and 2002 have drawn considerable public attention and raised communal debate about the topic.

Despite the strong demand for a good system for water quality monitoring in the region, the complexity of the archipelago makes its planning particularly challenging. Until recently, monitoring has been mainly based on laboratory analyses of water samples collected from fixed sampling locations (Kirkkala et al., 1998; Hänninen et al., 2000). However, the vast expanse and highly dynamic nature of the region make this technique too time-consuming and expensive. It is also unable to reflect the fine-scale water currents that may challenge water quality patterns gained through point data interpolation. A new basis and new tools for monitoring are thus called for.

Remote sensing technologies provide some promising possibilities to meet this need. Sea water studies using remote sensing have mostly been applied using data from sea satellites such as the SeaWiFS (Kahru and Mitchell, 1999) or weather satellites, particularly satellites from the National Oceanic and Atmospheric Administration (NOAA) (Kahru et al., 1994; Semovski et al., 1999). Data from these satellites have been used to detect for example sea surface temperature, turbidity, chlorophyll and cyanobacterial blooms (e.g. Kahru et al., 1994; Kahru and Mitchell, 1999; Semovski et al., 1999). None of these coarse spatial resolution data types are, however, suitable for the monitoring of such a fine-scaled mosaic as that which prevails in the coastal archipelago. Data from satellites with higher ground resolution, despite being designed for terrestrial applications, have been successfully used to quantify water quality parameters and turbidity patterns in some areas (Bagheri and Dios, 1990; Baban, 1997; Lira et al., 1997) and possess the potential for relatively fine-scale surface water pattern monitoring (Khorram et al., 1991; Forster et al., 1993; Tassan, 1993; Pattiaratchi et al., 1994; Ruiz-Azuara, 1995). As to the Baltic Sea, remote sensing has been mainly used in open sea conditions (e.g. Ekstrand, 1992; Semovski et al., 1999; Siegel et al., 1999), and only a few experimental tasks have been done in the Archipelago Sea (Kutser et al., 1998; Härmä et al., 2001). Consequently, this sea region lacks systematic surveys of surface water patterns with the use of the space-borne remote sensing technologies currently available.

The present study aims to explore these questions using data from the Landsat satellites representing six late summer situations in the 1990s. By the months of July and August the coastal aquatic ecosystem has reached its maximum level of summer-time biological production. In addition, in these months the negative consequences of eutrophication (e.g. coastal cyanobacterial blooms, mats of filamentous algae) are most problematic for the residents of the coastal region. For these reasons, the in situ samplings of the water quality monitoring programmes are usually scheduled for this time of the year. Here, the spatial and temporal surface water patterns are explored as viewed in the satellite images, and these results are compared with the pattern found in reference data from long-term water quality monitoring analyses. The aim is also to understand the dynamics of the surface waters within this region better, in order to come up with an appropriate strategy for an integrated water quality monitoring system, specifically designed for the complex conditions of the Archipelago Sea.

2. Materials and methods

2.1. The study area

The Archipelago Sea is a sub-region of the Baltic Sea, which is a non-tidal, semi-enclosed brackish water basin connected to the North Sea and the Atlantic Ocean through narrow straits (Fig. 1). Among the most peculiar characteristics of the Baltic Sea is the pronounced density stratification of its waters, related to salinity and temperature distribution (Kullenberg, 1981). Seasonality with annual variations prevails in the Baltic: during the summer peak surface water temperatures exceed +20 °C and in winter at least partial ice cover is developed (HELCOM, 1993).

The study area comprises the majority of the Southwestern Finnish Archipelago (Fig. 1). The spatial extent of the Archipelago Sea is over 9000 km^2 and it constitutes a topographically complex scheme of an old peneplain that is tilted westwards, thus giving rise to an archipelago where over 22 000 islands are found. Characterised by post-glacial isostatic land uplift with an annual rate of 4–5 mm, the Archipelago Sea exhibits continuous formation of new islands in the outer zone and frequent joining together of existing ones in the inner archipelago (Granö and Roto, 1989; Tolvanen

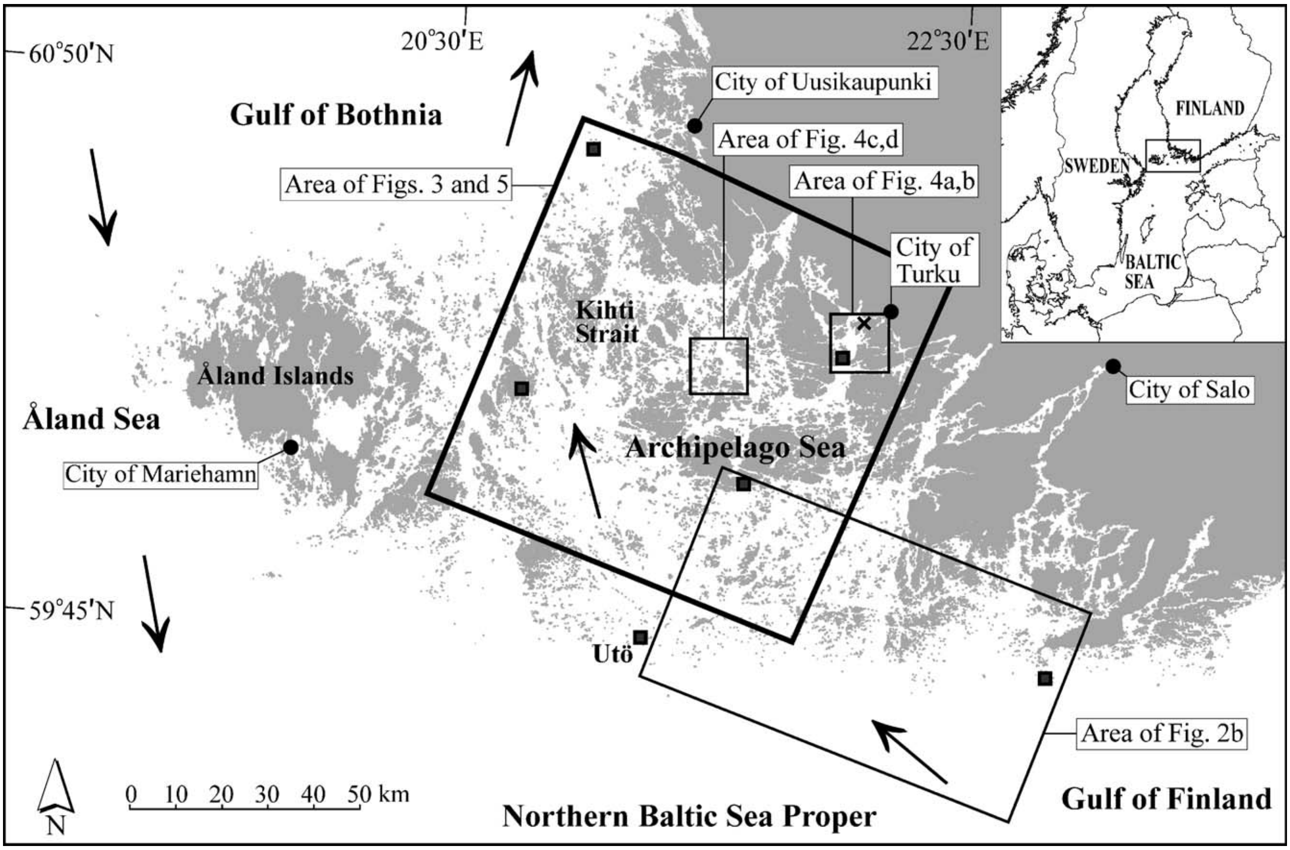

Fig. 1. The location of the Archipelago Sea of SW Finland. Quadrangles show the areal extent of: (a) the area of PCA1 and TM/ETM+ band 6 scenes in Figs. 3 and 5; (b) the southern border area in between the archipelago and open sea areas (Gulf of Finland) shown in Fig. 2b; (c) the area of Fig. 4a and b; (d) the area of Fig. 4c and d. Arrows indicate the general surface water flow model of the northern Baltic (source: HELCOM, 1993). Five square-shaped symbols show the sites of meteorological stations and the cross marks the hydrological station at Ruissalo.

et al., in press). Four geographical zones parallel to the coast are usually distinguished in this region (Häyrén, 1948; Granö, 1981): the outermost zone with rocky skerries; the outer zone with larger islets; the central archipelago with large islands and shallow waters; and the innermost zone with large islands similar to the mainland with narrow and shallow water straits between them.

In generalized flow models, surface waters circulate counter-clockwise throughout the Baltic Sea (HELCOM, 1993). Along the northern coast of the Gulf of Finland, westerly flow directions abound, and in the Archipelago Sea and eastern side of the Gulf of Bothnia a northward drift is prevalent (Fig. 1). Having large areas less than 10 m deep and an average water depth of 23 m, with the deepest trench reaching 146 m, the Archipelago Sea can be considered a particularly shallow sea area (Kirkkala et al., 1998). The presence of some relatively deep, north–south-directed bedrock fractures located in between the Archipelago Sea and the Åland Islands, facilitates a through-flow of waters between the Gulf of Bothnia and the Baltic Sea proper (Helminen et al., 1998). In the archipelago, fluctuations in the direction and/or velocity of the sea currents are pronounced due to the synergism of numerous factors, e.g. coastal morphology, wind disturbance, seiches, and mixing of termohaline layers (Virtaustutkimuksen neuvottelukunta, 1979; Kullenberg, 1981).

2.2. Landsat images and image acquisition conditions

The criteria used in searching satellite images from the archives of Eurimage included extensive temporal coverage, conditions of high summer and maximally cloud-free spatial cover. To achieve maximum temporal coverage only the central archipelago region covered by both Landsat paths 190 and 191 in row 18 were considered (Fig. 1). Acquisition dates close to the days of available water quality monitoring data were preferred, but only a few coinciding days of field sampling and image acquisition were found. The final selection of images (Table 1) includes four Landsat TM-images and two ETM+-images, both path-oriented with radiometric and geometric corrections, using the nearest neighbourhood method.

Water level data and surface water temperatures come from the hydrographical stations near the city of Turku, mainly the station at Ruissalo. Water temperatures range at the times of image registration between

Table 1
Satellite images used in the study with hydrographical and meteorological information related to each image's acquisition

Acquisition year	1996	1996	1997	1997	1999	1999
Acquisition date	6 August	13 August	9 August	16 August	29 July	7 August
Acquisition time, UTC (hh.mm)	08.57	09.04	09.13	09.19	09.41	09.34
Landsat satellite and sensor	L5 TM	L5 TM	L5 TM	L5 TM	L7 ETM+	L7 ETM+
Path—row	190—18	191—18	190—18	191—18	191—18	190—18
Image quality	D	B	B	A	B	C
Water temperature (+ °C)	18.9	20.2	21.9	19.0	19.8	19.8
Visibility in Utö (km)	30	25	30	30	25	30
Temperature sum > +5 °C, Turku	751.7	842.4	1014.1	1092.1	888.6	1012.7
Temperature sum > +5 °C, Utö	565.8	661.0	893.7	984.1	729.1	853.9
General wind directions: past 12 h	N–E	E–NE	S–SE	N	W–NW	N
Wind velocities (m s^{-1}): past 12 h	1–5	1–6	1–5	3–8	4–8	1–9

Local summer-time is UTC + 3 h. Image quality codes are: A = no cloud cover, B = insignificant cloud cover, C = partially covered by clouds/haze, D = major areas covered by clouds/haze. Data on sea water are from the station at Ruissalo except in 1996, when data are from the Finnish Environmental Administration's nearby sampling location "Turm 210". Climatological information has been generalized using data from weather monitoring stations located in the study area (see Fig. 1). Data sources: Finnish Institute of Marine Research, Finnish Environmental Administration and Finnish Meteorological Institute.

+18.9 °C and +21.9 °C. In the image acquisition times, the water level varied within the range of +10 cm to −27 cm from zero-level, with a tendency to a slight decrease during the last three days in most of the image acquisition periods (Finnish Institute of Marine Research, unpublished data). The sum of accumulated temperatures, a measure reflecting the status of the growing season from the 1st of May, varies considerably between the image acquisition dates and is always lower in the outer archipelago (Utö) than in the coastal mainland (Turku).

Data concerning wind direction and velocity were used from five meteorological stations located in the region (Fig. 1). The image acquisition days were generally calm with moderate winds, but stronger wind speeds may have occurred during some of the preceding days. In spite of the fact that the prevailing wind direction in the archipelago is from the west and southwest (Virtaustutkimuksen neuvottelukunta, 1979), wind directions ranged considerably both at the time of image acquisition and during the preceding days.

2.3. Image processing

Image processing was performed in the Laboratory of Computer Cartography of the University of Turku using ERDAS IMAGINE 8.4 software (Erdas, Inc., 1999). The image acquired on 6 August 1996 was rectified to the Finnish national grid using GCP points collected from the digital nautical chart of the Finnish Marine Administration and the remaining images were rectified to that image on an image-to-image basis. Although the total root mean square errors in image rectifications remained below 0.5, minor discrepancies were found between the rectified images, particularly in areas of small islets and a complex shoreline, where the local conditions may vary among the images. Finally, subsets for the study area were cut from the rectified images. Atmospheric correction was not performed, because simultaneous radiometric measurements were not available. Since Baltic Sea waters are turbid with high concentrations of yellow substances, general atmospheric correction methods developed for coastal waters are not reliable.

In order to concentrate image analysis efforts on water areas only, masks were created for this purpose. Each image was thresholded, defining reflectance values over 20 in band 5 (TM and ETM+) as land (see Earth Resource Mapping Pty Ltd., 1995). Although the digital numbers of the different sensors are not identical and no atmospheric corrections were made, the thresholding was found to produce satisfactory results. Masks for inland water, clouds and their shadows were created manually. The land and cloud mask images were joined through raster value summation separately for each image. In the masks, value 1 corresponded to water and value 0 to land or clouds, resulting in a pixel value of 2 only in the case of water pixels. Later, water pixels were given the value 1 in contrast to value 0 for all other pixels, thus making it possible to create a uniform water mask, by merging the six separate masks for another raster summation, with pixel value 6 in the resulting image being assigned to water. The resulting mask was independent of the contribution of single clouds or exceptional shoreline patterns in some of the original images.

In order to reduce image noise and enhance spatial patterns, focal mean filtering was performed for each masked image. In the fragmented archipelago, a 3 × 3 pixel array was found applicable as it fades out image banding slightly, but still the surface water patterns remain fairly unchanged.

2.4. Spectral image analyses

Water patterns and flow forms were studied first through visual interpretation of grey-scale images of all

TM/ETM+ bands. In accordance with literature sources (Baban, 1993; Dekker and Peters, 1993; Fraser, 1998), the TM and ETM+ visible bands 1–3 (450–520 nm, 520–600 nm, 630–690 nm, respectively) were found to contain most information on the spatial distribution of surface waters. These bands are in the visible portion of the electromagnetic spectrum, where spectral reflectance from water surfaces occurs. The spectral reflectance of the water surface is a result of underwater absorption and scattering processes. In natural waters, the most important components affecting the absorption and scattering processes are the water itself, suspended inorganic and organic matter, phytoplankton pigments and colored dissolved organic matter (van Stokkom et al., 1993), with the term turbidity referring to their combined influences. In these bands, the spectral information is a mixture of the absorption and scattering processes of optically active components. Chlorophyll-*a* absorbs irradiance in the blue and red portions of the visible wavelengths, whilst dissolved aquatic humus absorbs strongly in the shorter wavelengths (i.e. blue portion of visible wavelengths). Backscattering from all the suspended particles decreases in the near-infrared wavelengths, where absorption caused by the water itself strongly increases (e.g. Dekker et al., 1992; Dekker and Peters, 1993).

Principal component analyses (PCA) using the TM/ETM+ bands 1–3 were performed for each image in order to concentrate their most important information content into one layer and thus facilitate the recognition of their spatial patterns. The thermal infrared band (TM6, 10.42–12.50 μm) appeared to express somewhat different patterns in the surface waters, thus it was considered separately in flow pattern analyses. Special attention was paid to recognising the edges of surface water bodies, spectrally distinctive water areas and plume-like current forms.

The consistency of the surface water patterns of the visible wavelengths in the region was studied by creating an 18-banded combination image from the original TM/ETM+ bands 1–3 of the images. Unsupervised classification using the ISODATA clustering method was employed for the combination image formed from the original bands used for first principal component analysis, with the convergence threshold set at 0.95, the standard deviation set at 1 and the number of classes defined as 10. The ISODATA is an iterative method that repeatedly performs an entire classification until, in this case, 95% of the pixels remain unchanged between two successive steps (Erdas, Inc., 1999). The colors of the resulting clusters were assessed to correspond to a gradient from the open sea to the coast, yet it is not possible to connect them directly with any single water quality parameter.

2.5. Water quality parameters

Information on water quality was obtained from the Southwest Finland Regional Environment Centre (data source: Finnish Environment Administration). Because few if any of the water samplings had been performed at the times of the image acquisition dates, their usefulness in direct comparisons between the water quality data and single images remains limited. Therefore, average values of the water quality data are used, representing the summer from May to September during the years 1995–1999. The sampling sites represent the study area ($N = 45$) and adjacent sea areas ($N = 39$). The amount of sampling times over the years varies from three to over a hundred in different locations. Only the parameters describing the turbidity and general trophic status of the water column are considered: Secchi disk depth and chlorophyll-*a*. These measurements are made on every sampling occasion, and chlorophyll-*a* is measured from composite samples collected from depths of 0–10 m. Because water quality parameters were not available from the days of image acquisition, their values should be linked with caution to the patterns that are discernible in the studied imagery.

3. Results

3.1. Surface water reflectance patterns

In a broad view of the Archipelago Sea and its adjacent sea areas, the satellite images show pronounced spatial patterns in surface water reflectance (Fig. 2a). Two water areas show especially high reflectance of visual light: the mainland coast and the shores of the largest islands (Åland Islands). Also, the water areas in their vicinities show relatively high reflectance values, while in the open sea the reflectance values are lower. Characteristic to the open sea, rounded fluid patterns in the surface water are widely present, with their radius ranging up to tens of kilometres. In Fig. 2b, fluid spirals in the open sea are particularly noticeable in the Gulf of Finland, probably consisting of cyanobacterial drifts. Entering from the Gulf of Finland, these algal drifts reach the southernmost outer archipelago where local sources of eutrophication are few. The rounded fluid patterns fade away in this area where pelagic openness gives way to a labyrinth of islands and relatively shallow bodies of water.

Multi-temporal imagery shows consistent high reflectance values for both the coastal region in general and the narrow bays, straits and semi-closed bodies of water in the archipelago in particular (Fig. 3). However, major differences in the patterns of high and low reflectance values can also be seen. Each time snapshot shows its unique circumstances both regionally and as

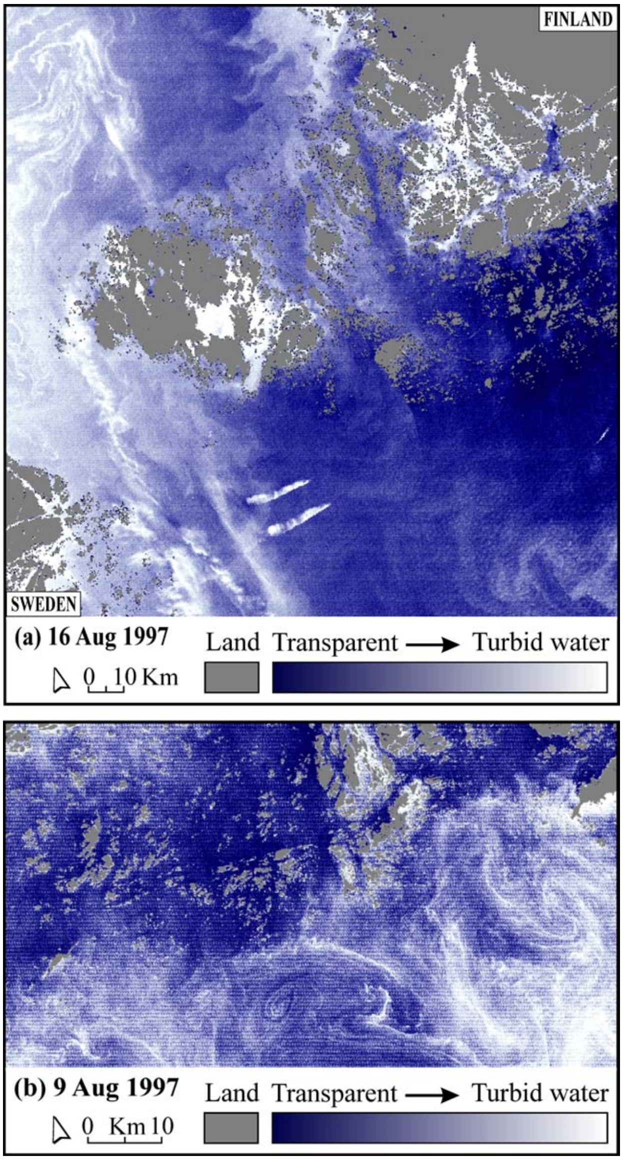

Fig. 2. Large-scale surface flow patterns in the northern Baltic Sea. (a) Overview of the Archipelago Sea and its nearby sea areas according to the Landsat TM-image acquired on 16 August 1997 (band 1, 3 × 3 low pass filter). (b) Detail of pattern in the Gulf of Finland during putative cyanobacterial bloom period (9 August 1997, Landsat 5 TM, band 1, 3 × 3 low pass filter). In both images, the light tones indicate turbid surface water.

forms indicating water currents and mixing. In some images (Fig. 3b and c), the outer southern archipelago presents higher values than the central archipelago, possibly as a result of algal drifts from the open sea.

The comparison of small-scale details in images acquired at different times challenges any view obtained from a single image examination especially in the central archipelago: a variety of dynamic fluid forms can be found in the very same places at different times (Fig. 4; see also Fig. 3). An example of such dynamism in Fig. 3 is the Kihti Strait that forms a north–south directed corridor through the archipelago. It often has less turbid waters than its sides, both east and west, but the flow direction in the strait varies from time to time, as shown by patterns in its contact and mixing zone with the adjacent sea areas (e.g. Fig. 3d and f).

Thermal infrared images (Fig. 5) confirm major spatial and temporal variations in the surface temperatures within the archipelago, often dissimilar to those shown in the visual bands of the same image. The warmest waters are usually found in closed sea basins and in bays near the mainland, whereas the coldest waters are usually found in the open sea. Patch-like cold-water occurrences within the archipelago are frequently discernible in the images. These features may suggest local short-term upwelling events, related to the prevailing wind direction of the past few days. For example, northerly winds had prevailed for a few days before 16 August 1997 and as a consequence, major areas of cold water occur in the Gulf of Bothnia (Fig. 5d). In contrast, in some images the thermal patterns across the Archipelago Sea appear relatively homogeneous as a consequence of the warming-up of surface waters during the calm days that had preceded the image acquisition dates (Fig. 5c).

3.2. Permanency of average water conditions

Unsupervised classification based on multi-temporal imagery conveys more or less stable patterns of general water turbidity, which occur as zones from the coastal region toward the open sea (Fig. 6). In most parts of the archipelago, the water zones are seen as relatively wide belts, whilst in the northern areas turbid coastal waters change to those of the open sea within short distances. In the southern archipelago, despite some occasions of putative algal bloom, frequently turbid waters are rare. Patterns shown by the unsupervised classification also suggest that the southern and northern (north-western) parts of the outer archipelago are on average dissimilar, the southern end of the Kihti Strait acting as an important divider between the average water types.

The classes obtained through unsupervised classification coincide with the registered water quality parameters (Fig. 6). The correlation coefficient of the unsupervised classification with Secchi disk depth is −0.890, while with chlorophyll-*a* it is 0.436 ($p < 0.05$, $N = 45$). Several factors affect the optical properties of a water column with varying intensity and contribute to the Secchi disk depth measurements. When chlorophyll-*a* is low, sources other than phytoplankton may cause turbid waters (e.g. inorganic suspension particles).

The areas nearest to the mainland and by some large solitary islands represent the most turbid waters in the region, usually with Secchi depths of less than 2 m. Progressing outwards, the average Secchi depths increase

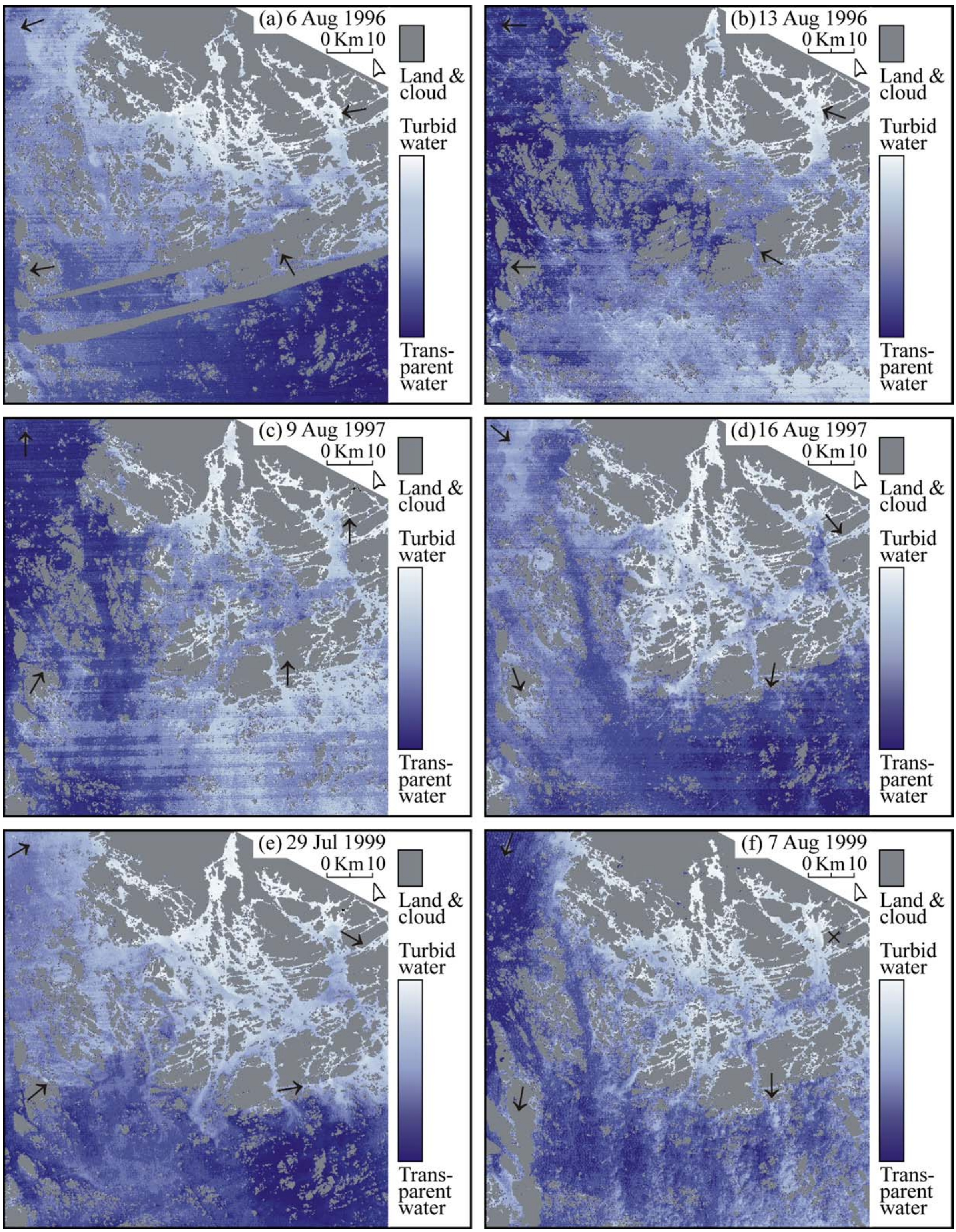

Fig. 3. Spatial patterns of spectral reflectance in the Archipelago Sea in six late summer images (first principal component of TM/ETM+ bands 1–3). The lightest shade of blue indicates the highest PC 1 values and the darkest shade of blue stands for the lowest values. Land and clouds are grey. Colors are not calibrated between the individual images. Arrows show the wind direction in the meteorological stations on the respective dates at noon.

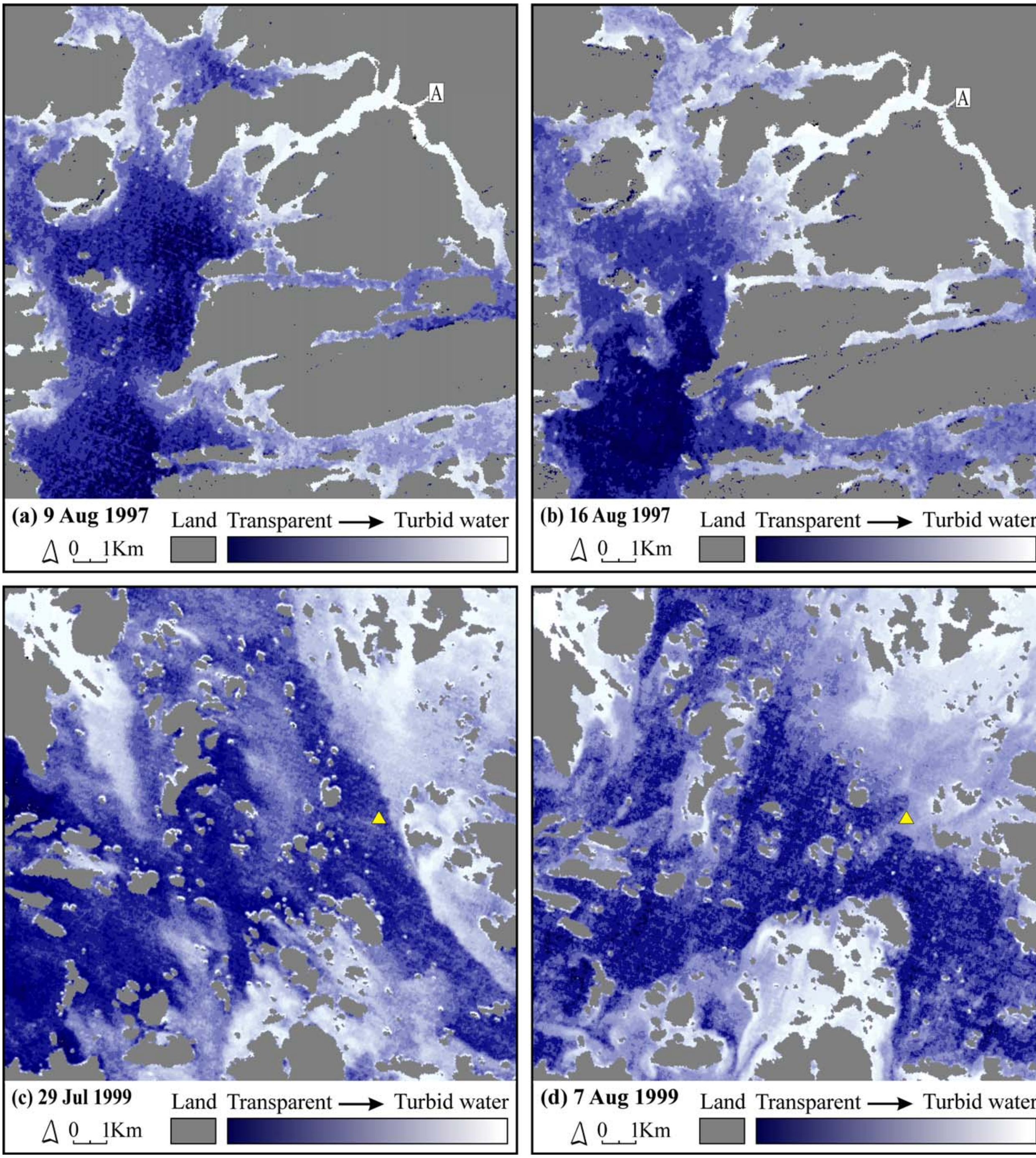

Fig. 4. Details of the images presented in Fig. 3 (for information on locations, see Fig. 1). The mouth of river Aurajoki is marked with letter A. Yellow triangle marks the location of a long-term sampling site, "Rym 390".

gradually up to ca. 3–5 m in the open sea. In accordance with the lowest Secchi depth values, the highest concentrations of chlorophyll-*a* are found in the innermost archipelago, particularly by mouths of rivers (Fig. 6b). In the narrow straits and shallow bays of the inner archipelago, chlorophyll-*a* concentrations reach values above $4\,\mu g\,l^{-1}$. Chlorophyll-*a* also shows a tendency to be slightly higher in the south-eastern part of the archipelago ($3-4\,\mu g\,l^{-1}$) in comparison with the inner and central archipelago areas ($2-3\,\mu g\,l^{-1}$). In the outer archipelago, the average concentrations of chlorophyll-*a* in the sampling sites are more uniform than those in the central archipelago where adjacent sampling sites may present significantly different values.

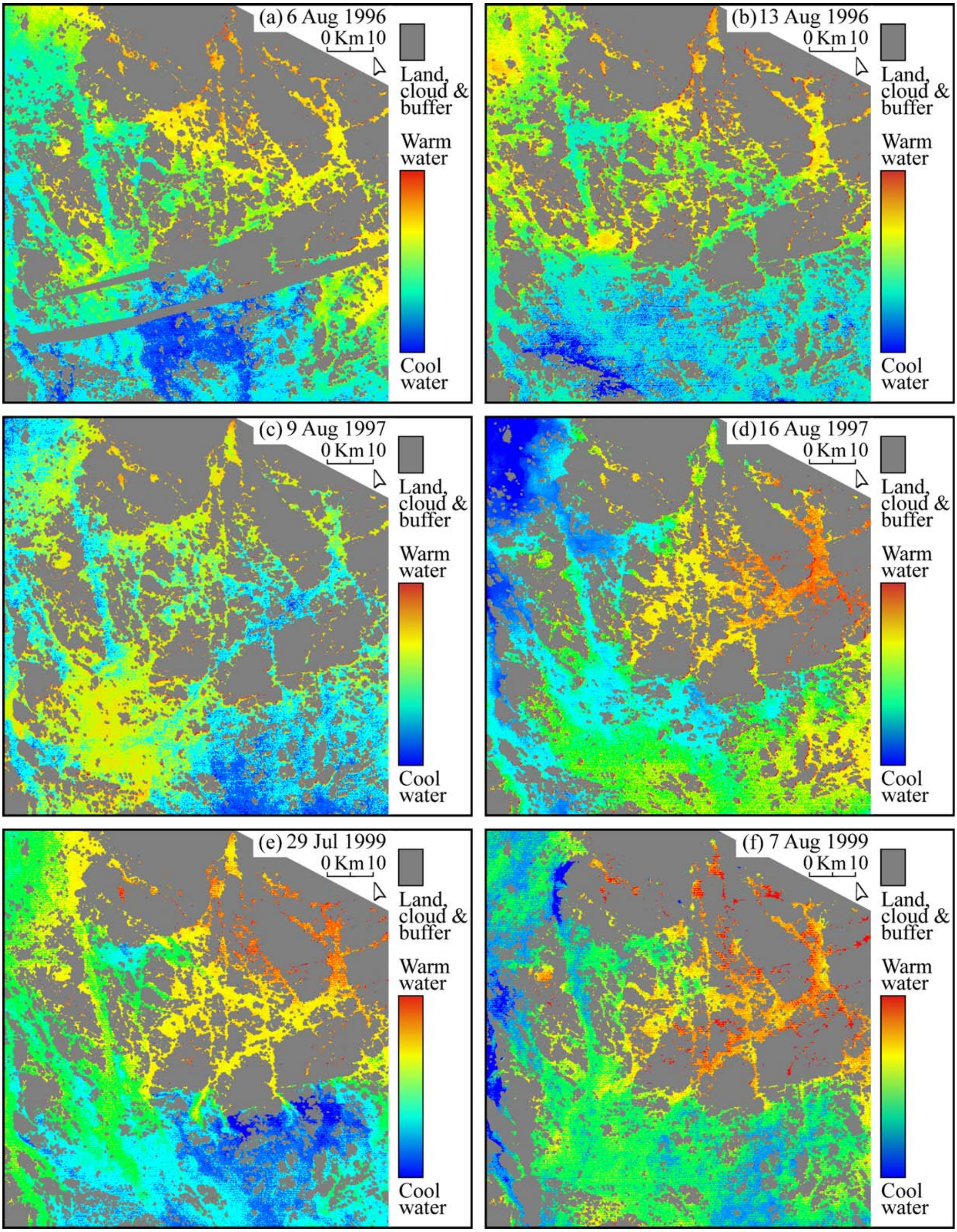

Fig. 5. Spatial patterns of spectral reflectance of TM/ETM+ band 6 (thermal infrared). On the image is a grey buffer layer of 200 m in length round the shoreline, thus preventing the locally warm littoral areas from showing. The colors are not comparable in terms of absolute temperature, but are relative; red showing the warmest areas and darkest shade of blue the coldest surface waters. Land and clouds are grey. For information on water temperatures, see Table 1 and for wind directions, see Fig. 3.

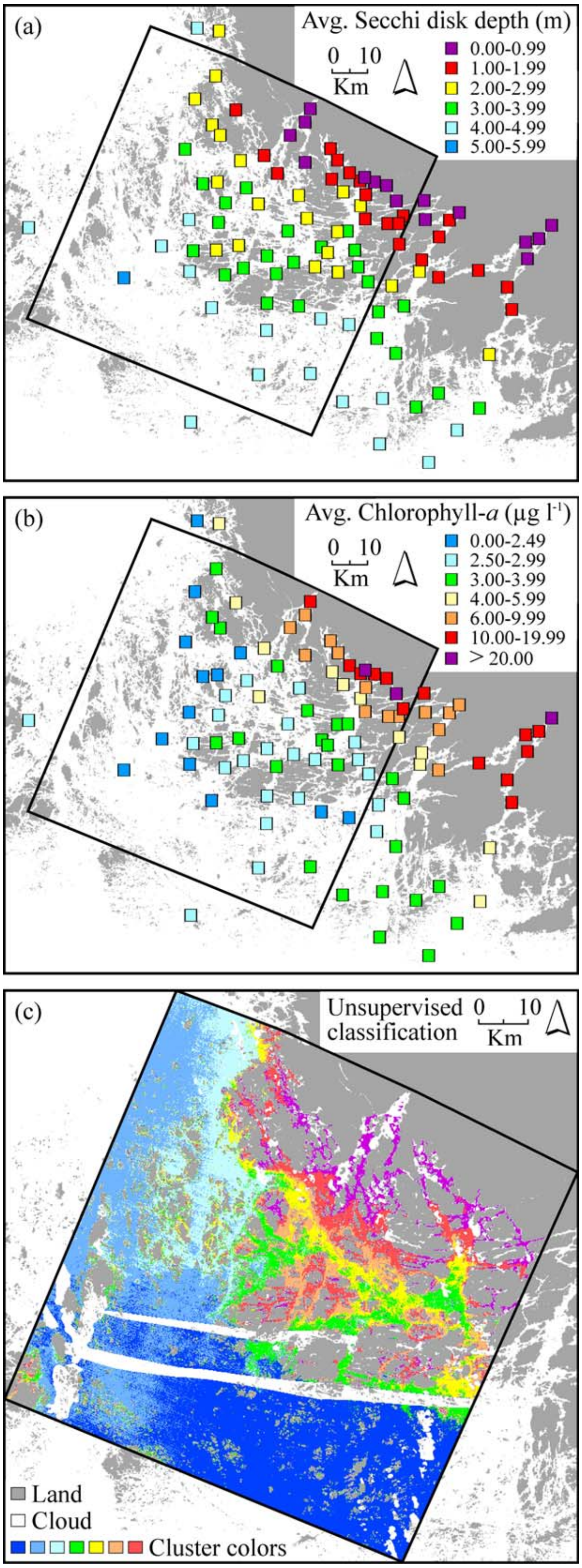

Fig. 6. Average water conditions in the Archipelago Sea according to filed sampling and multi-temporal satellite imagery. (a) Average Secchi disk depth distribution. (b) Average chlorophyll-*a* distribution. (c) Unsupervised classification based on data from TM/ETM+ bands 1–3 from six late summer Landsat images. Water areas are disturbed by clouds (white color).

4. Discussion

4.1. Surface water dynamics

The patterns and dynamics of the surface waters discernible in the remotely sensed data under study evidence a variety of non-persistent currents in the Archipelago Sea. Acting as a mixing zone for runoff from the mainland and waters coming from the adjacent sea areas, temporal currents and amalgamation of water masses occur in various parts of the area. According to these observations, the surface water quality in many parts of the region may change radically within short periods of time, particularly in the central and outer archipelago. In the archipelago interior, the least turbid waters are usually found in relatively deep areas of open sea. Where groups of large islands occur with narrow straits between, turbid waters often occur but the constancy of this phenomenon varies from time to time. Some groups of islands sustain turbid waters in certain images whilst this phenomenon may be weak or non-existent at other times. During calm periods, surface water temperatures across the region may show rather uniform patterns but water turbidity remains diverse even during these days.

High reflectance values of visible light in the late summer images reveal high turbidity. Although no field data on the phytoplankton status are available from the image acquisition dates, it is assumed that, especially in the outer archipelago, the contribution of phytoplankton to turbidity is significant. Favourable conditions for free-floating algae typically develop in warm late summer waters (Kahru et al., 1994). In the southern archipelago, cyanobacterial drifts mainly originate from the Baltic Sea proper and the Gulf of Finland where late summer algal blooming is phenomenal (Finni et al., 2001). The patterns shown in the images are in accordance with both the counter-clockwise surface water flow model of the Baltic Sea (HELCOM, 1993) and recent studies concerning nutrient dynamics in the outer archipelago and open sea areas (e.g. Hänninen et al., 2000). The levels of total nitrogen and phosphorous are lowest in the outer archipelago, while in the Gulf of Finland the nutrient concentrations are at the levels of the central archipelago (Hänninen et al., 2000). Water exchange with the Baltic Sea proper appears to be of most importance in the southern archipelago, and likewise in the north-western archipelago, the Gulf of Bothnia may extend its influence deep into the archipelago (Helminen et al., 1998).

The currents in the Baltic Sea are primarily induced by varying meteorological phenomena and the main source of energy for the water motion and water level change are wind and air-pressure (Kullenberg, 1981; Granö and Roto, 1989). The cyclonical mean circulation velocities are weak, ca. 1 cm s^{-1} (Winterhalter et al., 1981). In the Archipelago Sea, the flow measurements conducted in some parts of the region (Virtaustutkimuksen neuvottelukunta, 1979) have shown currents moving back and forth in many narrow straits, often with frequent changes in flow direction. In the satellite images, many water exchange events in the region appear as plume- or wedge-shaped flow forms that are particularly visible in areas where turbid waters intrude into less turbid ones through a narrow strait. Thermal stratification in the summer hinders the vertical mixing of the currents with the bottom layer and the intricacy of this hydrodynamic system is further increased by the numerous basins and straits of this region (Virtaustutkimuksen neuvottelukunta, 1979). Indeed, some major straits formed in deep bedrock fractions are often less turbid than their adjacent waters, and they are important links of water exchange between the outer archipelago and its interior. The multi-temporal imagery used in this study also corroborates the fact that the surface water currents of the Archipelago Sea are highly capricious in nature: no evidence of consistent flow patterns was found.

Despite changeable currents, the general water turbidity pattern found in this study reveals a distinctive consistency. The gradient of water turbidity in the unsupervised classification of multi-temporal data is in accordance with previous observations concerning nutrient levels and sources in the region (Hänninen et al., 2000). Where human activities peak, turbid waters are usually found. Fish farming is the most significant peak source of nutrients in the central archipelago whilst in the mainland coast and near some large islands agriculture is an important source of nutrients (Hänninen et al., 2000). The innermost narrow bays by the mainland manifest constantly turbid waters with impeded water exchange, being also influenced by rivers rich in suspended sediments and dissolved nutrients (Hänninen et al., 2000). During the high summer, the runoff from these rivers is very low, in many cases less than 1 $m^3 s^{-1}$ (Finnish Environmental Administration, unpublished data). Even in these conditions, however, the wind-induced mixing of the thermal layers and resuspension of the bottom sediments in shallow bays with small water volume guarantee good availability of nutrients and along with high water temperatures creates favourable conditions for phytoplankton.

The general turbidity of the water column appears to have an explicit pattern with gradually increasing transparency towards the open sea (Fig. 6a). The sound correlation between the Secchi disk depth and the multi-temporal satellite-based classification (Fig. 6c) suggests that Landsat images efficiently pick up spatial patterns of the turbidity and possibly indirectly of the trophic status of the waters. Although both the composition of the water constituents and the flow regime change constantly, the gradual change from more turbid inshore areas and island groups to the more transparent open water areas is evident in the inner and central archipelago.

4.2. Implications for water quality monitoring

Regular surveillance of Finnish coastal water quality is performed by national, regional and local monitoring programmes, such as those related to municipal and industrial wastewater treatment plants and fish farming. Samples are collected by shipboard sampling from fixed locations, mainly in open water season with the emphasis on high summer. Surveillance is usually conducted a few times a year and the samples are subjected to a bulk of physical and chemical analyses, being measured vertically from different depths.

Plotted over the unsupervised classification image, the locations of the water sampling sites appear to represent the overall gradient of water turbidity satisfactorily. However, the central archipelago is poorly represented in relation to its large area and highly variable surface waters, and also the western and northern outer archipelago areas lack permanent field sampling. The number of sampling locations could be increased but due to the dynamic currents of the Archipelago Sea, a single water sample may not represent the conditions of even its immediate surroundings. A sampling network designed for the high summer realm may also fail to present a good picture of the spring and autumn situations, when river runoff and diffuse loading are higher, thermal stratification is absent and storms are frequent. However, it would be intolerably expensive to establish a significantly more representative water sampling regime for this region. On the contrary, the current economic atmosphere exerts pressure to reduce the number of permanently sampled sites. Due to this reality, traditional point sampling is and will remain insufficient in its ability to credibly reflect the water quality patterns prevailing in the central and outer archipelago areas. To reach a good cost–benefit ratio from investments made in field sampling, the integration of in situ data with remote sensing methods may provide interesting opportunities. In addition, basic scientific research on the local hydrographic realm and its behaviour, a dynamic model, would contribute to improved water quality monitoring. To overcome this problem, fluorometers have been installed in ships travelling in the Baltic Sea on a regular basis (Rantajärvi et al., 1998), but even this technique provides information from only narrow bands of the water.

Since it is able to visualize spatially comprehensive data, this study confirms that space-borne remote sensing can be considered a powerful tool to complement results from water analyses in the coastal archipelago. Landsat TM bands 1–3 show good correlation with water quality parameters in regression analyses

(Baban, 1993; Dekker and Peters, 1993; Fraser, 1998), and in turbid inland waters backscattering of suspended matter also occurs in band 4, although the absorption of water increases steeply beyond 850 nm (Dekker and Peters, 1993). The thermal bands of sensors onboard the Landsat satellites were also shown here to provide valuable information about dynamic surface flow patterns.

Because the local water quality patterns may change irregularly in the border areas of the turbidity zones, simultaneous field sampling and satellite data acquisition would be ideal. However, because the Baltic Sea has partial or full cloud cover 70% of the year (Kutser et al., 1998), data from space-borne remote sensing will hardly be able to accommodate these conditions. Airborne monitoring methods provide an alternative as they can also produce data on reasonably cloudy days but their limitation is that they represent rather narrow sectors only of the entire region. For example, a hyperspectral imaging spectrometer provides precise information of some water qualities (Härmä et al., 2001) and laser equipment installed onboard an aircraft can register different phytoplankton pigments (Babichenko et al., 1998, 1999). Using such methods, regular flights might be designed as transects from the inner to outer archipelago, concordantly with the water sampling dates. The feasibility of airborne remote sensing depends largely on the estimated cost–benefit ratio between the costs of the flights compared with water quality information achieved from the transect lines. Airborne remote sensing techniques do not, however, mean that satellite data are of no use. On the contrary, an effective water quality monitoring scheme requires integration of all levels of data acquisition, from space and airborne remote sensing methods to field sampling and hydrodynamic modelling (Kuittinen et al., 1991; Härmä et al., 2001).

The Archipelago Sea is a good example of a coastal region where a highly dynamic water flow regime and the need for an accurate monitoring methodology are encountered. Because the area is densely inhabited during the summer season and most recreational uses are related to the shores and the open sea, site-precise water quality information is of interest. The same reality also puts pressure on forecasting water conditions across the region, particularly during the high summer when leisure activities are at their peak and cyanobacterial drifts develop and migrate. The results of this study showed the usefulness of space-borne data in the identification of such phenomena, and their inclusion in future monitoring and forecasting programmes is to be expected.

5. Conclusions

Data from Landsat TM/ETM+ are able to express significant patterns of the dynamic surface waters of the Archipelago Sea, including gradual and abrupt changes in water quality and water flow forms. The bands of visible light expressing features of water turbidity present partially different patterns from those shown by data from thermal infrared. Both these data types are useful for dynamic water flow regimes such as those addressed in this study.

In the Archipelago Sea, surface currents play an important role in water exchange but they vary greatly in space and time depending on the preceding meteorological and hydrographical conditions at both regional and local scale. In particular, the central and outer archipelago areas present capricious flow patterns that still remain poorly understood. During high summer, the southern outer archipelago is highly influenced by incoming algal drifts from the Gulf of Finland and the Baltic Sea proper. Averaging the view of water turbidity by using images from different dates confirms that there are some permanently turbid areas in the region, particularly the inner archipelago in general, and also many narrow sea bays and straits with poor water exchange.

Effective water quality monitoring and forecasting in this type of environment requires a spatially large-scale view, which is gained efficiently using space-borne imagery. Large-scaled imageries are spatially complementary data sources, which can be efficiently incorporated into an integrated water quality monitoring and forecast system along with water sampling in the field, airborne surveillance, water quality modelling and hydrodynamic modelling.

Acknowledgements

The study was supported by the Maj and Tor Nessling Foundation, the Southwest Finland Regional Environment Centre, the Finnish Environment Institute and the Finnish Biodiversity Research Programme FIBRE. The authors wish to thank Timo Pyhälahti, Teija Kirkkala, Kari Kallio and Pekka Härmä for their valuable comments, Pasi Laihonen for fruitful discussions and Finnish Institute of Marine Research, Finnish Environmental Administration and Finnish Meteorological Institute for the data.

References

Baban, S.J., 1993. Detecting water quality parameters in the Norfolk Broads, U.K., using Landsat imagery. International Journal of Remote Sensing 14, 1247–1267.

Baban, S.M.J., 1997. Environmental monitoring of estuaries; estimating and mapping various environmental indicators in Breydon Water Estuary, U.K., using Landsat TM imagery. Estuarine, Coastal and Shelf Science 44, 589–598.

Babichenko, S., Poryvkina, L., Orlov, Y., Persiantsev, I., Rebrik, S., 1998. Fluorescent signatures in environmental analysis. In: Meyers, R.A. (Ed.), Encyclopedia of Environmental Analysis and Remediation. John Wiley & Sons, Inc., pp. 1787–1791.

Babichenko, S., Kaitala, S., Leeben, A., Poryvkina, L., Seppälä, J., 1999. Phytoplankton pigments and dissolved organic matter distribution in the Gulf of Riga. Journal of Marine Systems 23, 62–82.

Bagheri, S., Dios, R.A., 1990. Chlorophyll-*a* estimation in New Jersey's coastal waters using Thematic Mapper data. International Journal of Remote Sensing 11, 289–299.

Bonsdorff, E., Blomqvist, E.M., Mattila, J., Norkko, A., 1997. Coastal eutrophication: causes, consequences and perspectives in the archipelago areas of the Northern Baltic Sea. Estuarine, Coastal and Shelf Science 44 (Suppl. A), 63–72.

Dekker, A.G., Malthus, T.J., Wijnen, M.M., Seyhan, E., 1992. Remote sensing as a tool for assessing water quality in Loosdrecht lakes. Hydrobiologia 233, 137–159.

Dekker, A.G., Peters, S.W.M., 1993. The use of the Thematic Mapper for the analysis of eutrophic lakes: a case study in the Netherlands. International Journal of Remote Sensing 14, 799–821.

Earth Resource Mapping Pty Ltd., 1995. ER Mapper 5.0 Tutorial, pp. 1–286.

Ekstrand, S., 1992. Landsat TM based quantification of chlorophyll-*a* during algae blooms in coastal waters. International Journal of Remote Sensing 13, 1913–1926.

Erdas, Inc., 1999. Erdas Imagine Tour Guides. Erdas Imagine V8.4. Erdas, Inc., Atlanta, Georgia, pp. 1–636.

Finni, T., Kononen, K., Olsonen, R., Wallström, K., 2001. The history of cyanobacterial blooms in the Baltic Sea. Ambio 30, 172–178.

Forster, B.C., Xingwei, Sha, Baide, Xu, 1993. Remote sensing of sea water quality parameters using Landsat-TM. International Journal of Remote Sensing 14, 2759–2771.

Fraser, R.N., 1998. Multispectral remote sensing of turbidity among Nebraska Sand Hills lakes. International Journal of Remote Sensing 19, 3011–3016.

Granö, O., 1981. The zone concept applied to the Finnish coast in the light of scientific traditions. Fennia 159, 63–68.

Granö, O., Roto, M., 1989. The duration of shore exposure along the emerging Finnish coast. Journal of Coastal Research 5, 49–55.

HELCOM, 1993. First assessment of the state of the coastal waters of the Baltic Sea. Baltic Sea Environment Proceedings 54, 1–160.

Helminen, H., Juntura, E., Koponen, J., Laihonen, P., Ylinen, H., 1998. Assessing of long distance background nutrient loading to the Archipelago Sea, northern Baltic with a hydrodynamic model. Environmental Modelling and Software 13, 511–518.

Hänninen, J., Vuorinen, I., Helminen, H., Kirkkala, T., Lehtilä, K., 2000. Trends and gradients in nutrient concentrations and loading in the Archipelago Sea, Northern Baltic, in 1970–1997. Estuarine, Coastal and Shelf Science 50, 153–171. doi: 10.1006/ecss.1999.0568.

Härmä, P., Vepsäläinen, J., Hannonen, T., Pyhälahti, T., Kämäri, J., Kallio, K., Eloheimo, K., Koponen, S., 2001. Detection of water quality using simulated satellite data and semi-empirical algorithms in Finland. The Science of the Total Environment 268, 107–121.

Häyrén, E., 1948. Skärgårdens längszoner. In: Lindberg, H. (Ed.), Skärgårdsboken. Söderström, Helsinki (in Swedish), pp. 242–256.

Kahru, M., Horstmann, U., Rud, O., 1994. Satellite detection of increased cyanobacteria blooms in the Baltic Sea: natural fluctuation or ecosystem change? Ambio 23, 469–472.

Kahru, M., Mitchell, B.G., 1999. Empirical chlorophyll algorithm and preliminary SeaWiFS validation for the California Current. International Journal of Remote Sensing 20, 3423–3429.

Khorram, S., Cheshire, H., Geraci, A.L., La Rosa, G., 1991. Water quality mapping of Augusta Bay, Italy from Landsat-TM data. International Journal of Remote Sensing 12, 803–808.

Kirkkala, T., Helminen, H., Erkkilä, A., 1998. Variability of nutrient limitation in the Archipelago Sea, SW Finland. Hydrobiologia 363, 117–126.

Kuittinen, R., Sevola, P., Virtanen, M., 1991. Monitoring the Baltic Sea by remote sensing. Aqua Fennica 21, 95–103.

Kullenberg, G., 1981. Physical oceanography. In: Voipio, A. (Ed.), The Baltic Sea. Elsevier Oceanography Series, vol. 30. pp.135–181.

Kutser, T., Eloheimo, K., Hannonen, T., Härmä, P., Kirkkala, T., Koponen, S., Pulliainen, J., Pyhälahti, T., 1998. Monitoring of coastal waters of the Baltic Sea by airborne imaging spectrometer AISA. In: Brebbia, C.A. (Ed.), Environmental Coastal Regions. WIT Press, Southampton, pp. 123–134.

Lira, J., Morales, A., Zamora, F., 1997. Study of sediment distribution in the area of the Pánuco river plume by means of remote sensing. International Journal of Remote Sensing 18, 171–182.

Pattiaratchi, C., Lavery, P., Wyllie, A., Hick, P., 1994. Estimates of water quality in coastal waters using multi-date Landsat Thematic Mapper data. International Journal of Remote Sensing 15, 1571–1584.

Rantajärvi, E., Olsonen, R., Hällfors, S., Leppänen, J.-M., Raateoja, M., 1998. Effect of sampling frequency on detection of natural variability in phytoplankton: unattended high-frequency measurements on board ferries in the Baltic Sea. ICES Journal of Marine Science 55, 697–704.

Ruiz-Azuara, P., 1995. Multitemporal analysis of "simultaneous" Landsat imagery (MSS and TM) for monitoring primary production in a small tropical coastal lagoon. Photogrammetric Engineering & Remote Sensing 61, 187–198.

Semovski, S.V., Dowell, M.D., Hapter, R., Szczucka, J., Beszczyńska-Möller, A., Darecki, M., 1999. The integration of remotely sensed, seatruth and modelled data in the investigation of mesoscale features in the Baltic coastal phytoplankton field. International Journal of Remote Sensing 20, 1265–1287.

Siegel, H., Gerth, M., Neumann, T., Doerffer, R., 1999. Case studies on phytoplankton blooms in coastal and open waters of the Baltic Sea using Coastal Zone Color Scanner data. International Journal of Remote Sensing 20, 1249–1264.

van Stokkom, H.T.C., Stokman, G.N.M., Hovenier, J.W., 1993. Quantitative use of passive optical remote sensing over coastal and inland water bodies. International Journal of Remote Sensing 14, 541–563.

Tassan, S., 1993. An improved in-water algorithm for the determination of chlorophyll and suspended sediment concentration from Thematic Mapper data in coastal waters. International Journal of Remote Sensing 14, 1221–1229.

Tolvanen, H., Numminen, S., Kalliola, R. Spatial distribution and dynamics of special shore-forms (tombolos, flads and glo-lakes) in an uplifting archipelago of the Baltic Sea. Journal of Coastal Research, in press.

Virtaustutkimuksen neuvottelukunta, 1979. Saaristomeren virtaustutkimus. Virtaustutkimuksen neuvottelukunta, 265 pp. (in Finnish).

Winterhalter, B., Flodén, T., Ignatius, H., Axberg, S., Niemistö, L., 1981. Geology of the Baltic Sea. In: Voipio, A. (Ed.), The Baltic Sea. Elsevier Oceanography Series, vol. 30. pp. 1–121.